Supplementary Information for

Observing the collapse of super-Bloch oscillations in strong-driving photonic temporal lattices

Xinyuan Hu[a,#], Shulin Wang[a,#], Chengzhi Qin[a,*], Chenyu Liu[a], Lange Zhao[a], Yinglan Li[a], Han Ye[a], Weiwei Liu[a,d], Stefano Longhi[b,c,*], Peixiang Lu[a,d,*] and Bing Wang[a,*]

[a]*Wuhan National Laboratory for Optoelectronics and School of Physics, Huazhong University of Science and Technology, Wuhan 430074, China.*

[b]*Dipartimento di Fisica, Politecnico di Milano, Piazza Leonardo da Vinci 32, I-20133 Milano, Italy.*

[c]*IFISC (UIB-CSIC), Instituto de Fisica Interdisciplinary Sistemas Complejos, E-07122 Palma de Mallorca, Spain.*

[d]*Hubei Key Laboratory of Optical Information and Pattern Recognition, Wuhan Institute of Technology, Wuhan 430205, China.*

[#]These authors contributed equally to this work

[*]Corresponding authors:

C. Q. (email: qinchengzhi@hust.edu.cn),

S. L. (email: stefano.longhi@polimi.it),

P. L. (email: lupeixiang@hust.edu.cn),

B. W. (email: wangbing@hust.edu.cn).

Supplemental Section

Supplementary Note 1: Derivation of the time-averaging band structure.

By combining Eq. (3) and Eq. (4), we can derive the time-averaging effective band structure

$$\begin{aligned}\langle\theta_{\pm}(k)\rangle &= \frac{1}{M_{\mathrm{ac}}}\int_0^{M_{\mathrm{ac}}}\theta_{\pm}[k(m)]dm \\ &= \frac{1}{M_{\mathrm{ac}}}\int_0^{M_{\mathrm{ac}}}\cos(\beta)\cos[k+(N\omega_{ac}+\delta)m-E_{\omega}\cos(\omega_{ac}m+\varphi)]dm \\ &= \frac{1}{M_{\mathrm{ac}}}\int_0^{M_{\mathrm{ac}}}\cos(\beta)\cos[k+\delta m+N\omega_{ac}m-E_{\omega}\sin(\omega_{ac}m+\varphi+\pi/2)]dm\end{aligned} \tag{S1}$$

After letting $t = \omega_{\mathrm{ac}}m+\varphi+\pi/2$, one obtains

$$\begin{aligned}\langle\theta_{\pm}(k)\rangle &= \frac{1}{M_{\mathrm{ac}}}\int_0^{M_{\mathrm{ac}}}\theta_{\pm}[k(m)]dm \\ &= \frac{1}{2\pi}\int_0^{2\pi}\cos(\beta)\cos[k+\delta m+N(t-\varphi-\frac{\pi}{2})-E_{\omega}\sin(t)]dt \\ &= \frac{\cos(\beta)}{2\pi}\int_0^{2\pi}\{\cos[k+\delta m-N(\varphi+\pi/2)]\cos[Nt-E_{\omega}\sin(t)] \\ &\qquad -\sin[k+\delta m-N(\varphi+\pi/2)]\sin[Nt-E_{\omega}\sin(t)]\}dt\end{aligned} \tag{S2}$$

Taking into account that $J_N(E_\omega) = \int_0^{2\pi}\cos(Nt-E_\omega\sin t)dt$ and $0 = \int_0^{2\pi}\sin(Nt-E_\omega\sin t)dt$, one finally obtains

$$\langle\theta_{\pm}(k)\rangle = \mp J_N(E_{\omega})\cos(\beta)\cos\left[k+\delta m-N\left(\varphi+\frac{\pi}{2}\right)\right]\mp\frac{\pi}{2}. \tag{S3}$$

which is precisely Eq. (4) given in the main text.

Supplementary Note 2: Averaged and instantaneous wave packet dynamics during SBOs

In this section, we provide a representative example to compare the averaged and instantaneous wave packet dynamics during SBOs. Here, the amplitude-to-frequency ratio and the detuning are set as E_ω = 5.3 and $\delta = \pi/150$. Figures S1(a) and S1(b) illustrate the simulated and experimental wave packet evolutions during SBOs, respectively. One sees that the measured data agree well with the simulation. During SBOs, a giant averaged oscillation accompanied with slight swings can be observed.

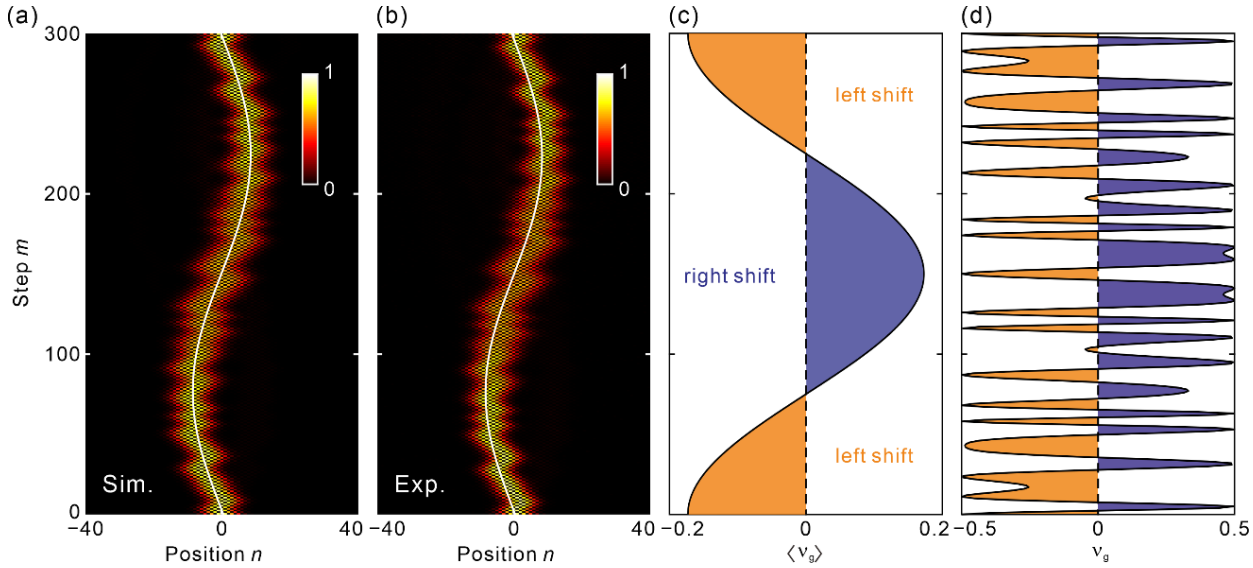

Fig. S1 Averaged and instantaneous wave packet dynamics during SBOs. (a), (b) Simulated and measured pulse intensity evolutions for E_ω = 5.3. (c) Averaged group velocity of wave packet during SBOs. (d) Instantaneous group velocity of wave packet during SBOs.

To explicitly analyze the wave packet dynamics during SBOs, we calculate the averaged and the instantaneous group velocities according to Eqs. (5) and (9). As depicted in Fig. S1(c), the averaged group velocity has a cosine function form along the propagation step m, reflecting a periodic oscillation of wave packet. At the first quarter of oscillation period $M_{\mathrm{SBOs}}/4$, the wave packet possesses a negative group velocity and thus shifts to the left side of lattice. The area of orange region denotes the modulus of the negative wave packet displacement. From the step $m = M_{\mathrm{SBOs}}/4$ to $m = M_{\mathrm{SBOs}}/2$, the group velocity becomes positive, reflecting the rightward motion of wave packet. As indicated by the purple region, the group velocity from $m = M_{\mathrm{SBOs}}/4$ to $m = M_{\mathrm{SBOs}}/2$ is opposite to the one from $m = 0$ to $m = M_{\mathrm{SBOs}}/4$, and the wave packet displacement is also opposite. Thus, the wave packet returns to its initial position at $m = M_{\mathrm{SBOs}}/2$. From $m = M_{\mathrm{SBOs}}/2$ to $m = M_{\mathrm{SBOs}}$, one can first observe a rightward wave packet

motion and then a leftward retrieval. Hence, within the period M_{SBOs}, a periodic oscillation of wave packet can be realized. Figure S1(d) depicts the instantaneous wave packet group velocity. One sees that the group velocity rapidly changes with the step m, which gives rise to the fast-varying swings during SBOs. At the first and last quarter of period M_{SBOs}, the net displacement of wave packet is negative, corresponding to the negative averaged group velocity. From $m = M_{\mathrm{SBOs}}/4$ to $m = 3M_{\mathrm{SBOs}}/4$, the wave packet possesses a positive net displacement and thus a positive group velocity.

Supplementary Note 3: Derivations of generalized SBOs under rectangular- and triangular-wave ac-driving fields.

We introduce a rectangular-wave ac electric field combined with a dc electric field $N\omega_{\mathrm{ac}}$

$$E_{\mathrm{eff}}(m)=\begin{cases} N\omega_{\mathrm{ac}}+\delta+E_{\mathrm{ac}}, & m\in[0,M_{\mathrm{ac}}/2) \\ N\omega_{\mathrm{ac}}+\delta-E_{\mathrm{ac}}, & m\in[M_{\mathrm{ac}}/2,M_{\mathrm{ac}}) \end{cases} \tag{S4}$$

To take a negative integral of E_{eff}, we obtain the vector potential

$$A_{\mathrm{eff}}(m)=\begin{cases} -N\omega_{\mathrm{ac}}m-\delta m-E_{\mathrm{ac}}m, & m\in[0,M_{\mathrm{ac}}/4) \\ -N\omega_{\mathrm{ac}}m-\delta m+E_{\mathrm{ac}}m-E_{\mathrm{ac}}M_{\mathrm{ac}}/2, & m\in[M_{\mathrm{ac}}/4,3M_{\mathrm{ac}}/4) \\ -N\omega_{\mathrm{ac}}m-\delta m-E_{\mathrm{ac}}m+E_{\mathrm{ac}}M_{\mathrm{ac}}, & m\in[3M_{\mathrm{ac}}/4,M_{\mathrm{ac}}) \end{cases} \tag{S5}$$

By averaging the instantaneous band structure within one ac-driving period M_{ac}, we arrive at the effective time-averaging band structure

$$\begin{aligned}
\langle\theta_{\pm}(k)\rangle &= \mp\frac{1}{M_{\mathrm{ac}}}\int_0^{M_{\mathrm{ac}}}\cos(\beta)\cos(k-A_{\mathrm{eff}})dm \\
&= \mp\frac{\cos(\beta)}{M_{\mathrm{ac}}}[\int_0^{\frac{M_{\mathrm{ac}}}{4}}\cos(k+\delta m+N\omega_{\mathrm{ac}}m+E_{\mathrm{ac}}m)dm \\
&\quad+\int_{\frac{M_{\mathrm{ac}}}{4}}^{\frac{3M_{\mathrm{ac}}}{4}}\cos(k+\delta m+N\omega_{\mathrm{ac}}m-E_{\mathrm{ac}}m+E_{\mathrm{ac}}M_{\mathrm{ac}}/2)dm \\
&\quad+\int_{\frac{3M_{\mathrm{ac}}}{4}}^{M_{\mathrm{ac}}}\cos(k+\delta m+N\omega_{\mathrm{ac}}m+E_{\mathrm{ac}}m-E_{\mathrm{ac}}M_{\mathrm{ac}})dm] \\
&= \mp\frac{\cos(\beta)}{M_{\mathrm{ac}}}[\cos(k+\delta m)\int_0^{\frac{M_{\mathrm{ac}}}{4}}\cos(dy_1)dm-\sin(k+\delta m)\int_0^{\frac{M_{\mathrm{ac}}}{4}}\sin(dy_1)dm \\
&\quad+\cos(k+\delta m)\int_{\frac{M_{\mathrm{ac}}}{4}}^{\frac{3M_{\mathrm{ac}}}{4}}\cos(dy_2)dm-\sin(k+\delta m)\int_{\frac{M_{\mathrm{ac}}}{4}}^{\frac{3M_{\mathrm{ac}}}{4}}\sin(dy_2)dm \\
&\quad+\cos(k+\delta m)\int_{\frac{3M_{\mathrm{ac}}}{4}}^{M_{\mathrm{ac}}}\cos(dy_3)dm-\sin(k+\delta m)\int_{\frac{3M_{\mathrm{ac}}}{4}}^{M_{\mathrm{ac}}}\sin(dy_3)dm] \\
&= \mp\cos(\beta)\{\frac{1}{2\pi(N+E_{\omega})}[\cos(k+\delta m)\int_0^{\frac{\pi(N+E_{\omega})}{2}}\cos(y_1)dy_1-\sin(k+\delta m)\int_0^{\frac{\pi(N+E_{\omega})}{2}}\sin(y_1)dy_1] \\
&\quad+\frac{1}{2\pi(N-E_{\omega})}[\cos(k+\delta m)\int_{\frac{\pi(N+E_{\omega})}{2}}^{\frac{3\pi N-\pi E_{\omega}}{2}}\cos(y_2)dy_2-\sin(k+\delta m)\int_{\frac{\pi(N+E_{\omega})}{2}}^{\frac{3\pi N-\pi E_{\omega}}{2}}\sin(y_2)dy_2] \\
&\quad+\frac{1}{2\pi(N+E_{\omega})}[\cos(k+\delta m)\int_{\frac{3\pi N-\pi E_{\omega}}{2}}^{2\pi N}\cos(y_3)dy_3-\sin(k+\delta m)\int_{\frac{3\pi N-\pi E_{\omega}}{2}}^{2\pi N}\sin(y_3)dy_3]\}
\end{aligned} \tag{S6}$$

where $y_1 = N\omega_{\mathrm{ac}}m+E_{\mathrm{ac}}m$, $y_2 = N\omega_{\mathrm{ac}}m-E_{\mathrm{ac}}m+E_{\mathrm{ac}}M_{\mathrm{ac}}/2$, and $y_3 = N\omega_{\mathrm{ac}}m+E_{\mathrm{ac}}m-E_{\mathrm{ac}}M_{\mathrm{ac}}$, which further leads to

$$\langle \theta_{\pm}(k) \rangle = \mp \frac{2E_{\omega}\sin[\pi(E_{\omega}+N)/2]}{\pi(E_{\omega}+N)(E_{\omega}-N)}\cos(\beta)\cos(k+\delta m). \tag{S7}$$

Correspondingly, the averaged group velocity can be calculated as

$$\langle v_{g,\pm}(k) \rangle = \mp \frac{2E_{\omega}\sin[\pi(E_{\omega}+N)/2]}{\pi(E_{\omega}+N)(E_{\omega}-N)}\cos(\beta)\sin(k+\delta m). \tag{S8}$$

Integrating the group velocity with respect to the evolution step m, we arrive at the averaged trajectory

$$\langle \Delta n_{\pm}(m) \rangle = \pm \frac{2E_{\omega}\sin[\pi(E_{\omega}+N)/2]}{\pi\delta(E_{\omega}+N)(E_{\omega}-N)}\cos(\beta)[\cos(k+\delta m)-\cos(k)], \tag{S9}$$

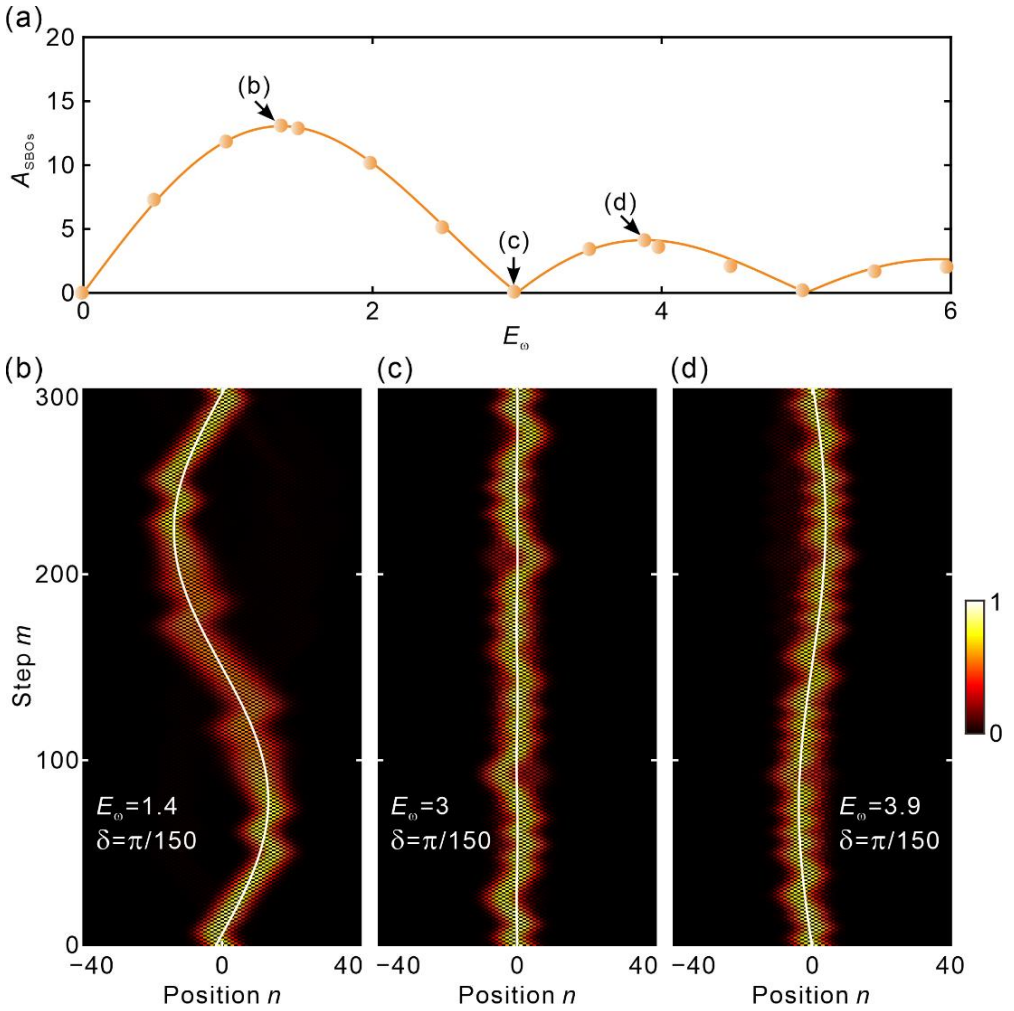

Fig. S2 Generalized SBOs under rectangular-wave ac-driving. (a) Oscillation amplitude A_{SBOs} varying with amplitude-to-frequency ratio E_{ω}. The solid curve and orange balls are the theoretical and experimental results, respectively. (b)-(d) Simulated pulse intensity evolutions for E_{ω} = 1.4, 3, and 3.9. The detuning is chosen as $\delta = \pi/150$.

Thus, the averaged trajectory of SBOs have a cosine form. When selecting the dc electric field $N\omega_{\mathrm{ac}}$ =

π/30 and the square-wave driving period M_{ac} = 60, the relationship between the oscillation amplitude A_{SBOs} and the amplitude-to-frequency ratio E_ω is shown in Fig. S2(a). The measured packet intensity evolutions for four different ac-driving amplitudes E_ω= 1.4, 3, and 3.9 cases are shown in Figs. S2(b)-2(d), which possess A_{SBOs} = 12.9, 0 and 3.6. Before the amplitude reaching the maximum point E_ω = 1.4 (Fig. S2(b)), the oscillation amplitude A_{SBO} increases with the increase of the ac electric field amplitude E_ω. As E_ω gradually increases, the oscillation amplitude shows a damping oscillation behavior. When reaching the first collapse point E_ω = 3 (Fig. S2(c)), the wave packet is localized around its initial position. Fig. S2(d) depict the wave packet evolution of SBOs after the collapse point (E_ω = 3.9), the amplitude of SBOs reappears and the initial phase of SBOs is opposite to the weak-driven case.

Then we consider a triangular-wave ac electric field combined with a dc electric field $N\omega_{ac}$

$$E_{\text{eff}}(m)=\begin{cases} N\omega_{ac}+\delta+E_{ac}-4E_{ac}m/M_{ac}, & m\in[0,M_{ac}) \\ N\omega_{ac}+\delta-E_{ac}+4E_{ac}(m-M_{ac}/2)/M_{ac}, & m\in[M_{ac}/2,M_{ac}) \end{cases} \tag{S10}$$

Since $E_{\text{eff}}(m) = -dA_{\text{eff}}(m)/dm$, the vector potential should be set as

$$A_{\text{eff}}(m)=\begin{cases} -N\omega_{ac}m-\delta m-E_{ac}m+2E_{ac}m^2/M_{ac}, & m\in[0,M_{ac}), \\ -N\omega_{ac}m-\delta m+E_{ac}(m-M_{ac}/2)-2E_{ac}(m-M_{ac}/2)^2/M_{ac}, & m\in[M_{ac}/2,M_{ac}). \end{cases} \tag{S11}$$

Then the effective band structure can be calculated as

$$\begin{aligned} \langle\theta_{\pm}(k)\rangle &= \mp\frac{1}{M_{ac}}\int_0^{M_{ac}}\cos(\beta)\cos(k-A_{\text{eff}})dm \\ &= \mp\frac{\cos(\beta)}{M_{ac}}\Big[\int_0^{\frac{M_{ac}}{2}}\cos(k+\delta m+N\omega_{ac}m+E_{ac}m-2E_{ac}m^2/M_{ac})dm \\ &\quad +\int_{\frac{M_{ac}}{2}}^{M_{ac}}\cos(k+\delta m+N\omega_{ac}m-3E_{ac}m+2E_{ac}m^2/M_{ac}+E_\omega M_{ac})dm\Big\} \end{aligned} \tag{S12}$$

we apply the formulas of trigonometric functions to separate the constant, and then use the perfect square for terms containing m

$$\begin{aligned}\langle\theta_{\pm}(k)\rangle = \mp\frac{\cos(\beta)}{\sqrt{2E_{\omega}}}\{&\cos(k+\delta m)[\cos(x)\int_0^{\frac{M_{ac}}{2}}\cos(\sqrt{2E_{ac}/M_{ac}}m-\sqrt{x})^2dm\\&+\sin(x)\int_0^{\frac{M_{ac}}{2}}\sin(\sqrt{2E_{ac}/M_{ac}}m-\sqrt{x})^2dm\\&+\cos(x_1)\int_{\frac{M_{ac}}{2}}^{M_{ac}}\cos(\sqrt{2E_{ac}/M_{ac}}m-\sqrt{x_1-E_{ac}M_{ac}})^2dm\\&+\sin(x_1)\int_{\frac{M_{ac}}{2}}^{M_{ac}}\sin(\sqrt{2E_{ac}/M_{ac}}m-\sqrt{x_1-E_{ac}M_{ac}})^2dm]\\&+\sin(k+\delta m)[\cos(x)\int_0^{\frac{M_{ac}}{2}}\sin(\sqrt{2E_{ac}/M_{ac}}m-\sqrt{x})^2dm\\&-\sin(x)\int_0^{\frac{M_{ac}}{2}}\cos(\sqrt{2E_{ac}/M_{ac}}m-\sqrt{x})^2dm\\&-\cos(x_1)\int_{\frac{M_{ac}}{2}}^{M_{ac}}\sin(\sqrt{2E_{ac}/M_{ac}}m-\sqrt{x_1-E_{ac}M_{ac}})^2dm\\&+\sin(x_1)\int_{\frac{M_{ac}}{2}}^{M_{ac}}\cos(\sqrt{2E_{ac}/M_{ac}}m-\sqrt{x_1-E_{ac}M_{ac}})^2dm]\}\end{aligned} \tag{S13}$$

where $x_1 = x - 2\pi N$. Using the Fresnel integrals $C(x)=\int_0^x\cos(t^2)dt$, $S(x)=\int_0^x\sin(t^2)dt$, we obtain the final result

$$\langle\theta_{\pm}(k)\rangle = \mp\frac{\cos(\beta)}{\sqrt{2E_{\omega}}}\{\cos(x)[C(x_+)+C(x_-)]-\sin(x)[S(x_+)+S(x_-)]\}\cos(k+\delta m). \tag{S14}$$

The effect of detuning δ is to make the Bloch momentum linearly sweep the Brillouin zone. The corresponding averaged group velocity is

$$\langle v_{g,\pm}(k)\rangle = \mp\frac{\cos(\beta)}{\sqrt{2E_{\omega}}}\{\cos(x)[C(x_+)+C(x_-)]-\sin(x)[S(x_+)+S(x_-)]\}\sin(k+\delta m). \tag{S15}$$

then the averaging trajectory of wave packet is obtained

$$\begin{aligned}&\langle\Delta n_{\pm}(m)\rangle = \int_0^M\langle v_{g,\pm}(k)\rangle dm\\&=\pm\frac{\cos(\beta)}{\delta\sqrt{2E_{\omega}}}\{\cos(x)[C(x_+)+C(x_-)]-\sin(x)[S(x_+)+S(x_-)]\}[\cos(\delta m+k)-\cos(k)],\end{aligned} \tag{S16}$$

As N = 1 and M_{ac} = 60, the oscillation amplitude A_{SBOs} as a function of the amplitude-to-frequency ratio E_{ω} is shown in Fig. S3(a). For $0 < E_{\omega} \leq 2.3$, the oscillation amplitude A_{SBO} increases with the increase of E_{ω}. At $E_{\omega} = 2.3$ (Fig. S3(b)), the amplitude A_{SBOs} reaches maximum. In the relatively strong ac-driving regime, i.e., $E_{\omega} \geq 2.3$, the oscillation amplitude shows a damping oscillation behavior with

the increase of the ac-driving strength. When $E_\omega = 4.8$ (Fig. S3(c)), the SBOs collapse with a vanished oscillation amplitude. For $E_\omega = 6$ (Fig. S3(d)), the wave packet initially oscillates from the opposite direction compared to the weak-driven case in Fig. S3(b). The SBOs is thus reversed, which is similar to the strong-driven SBOs under the sinusoidal-wave driving.

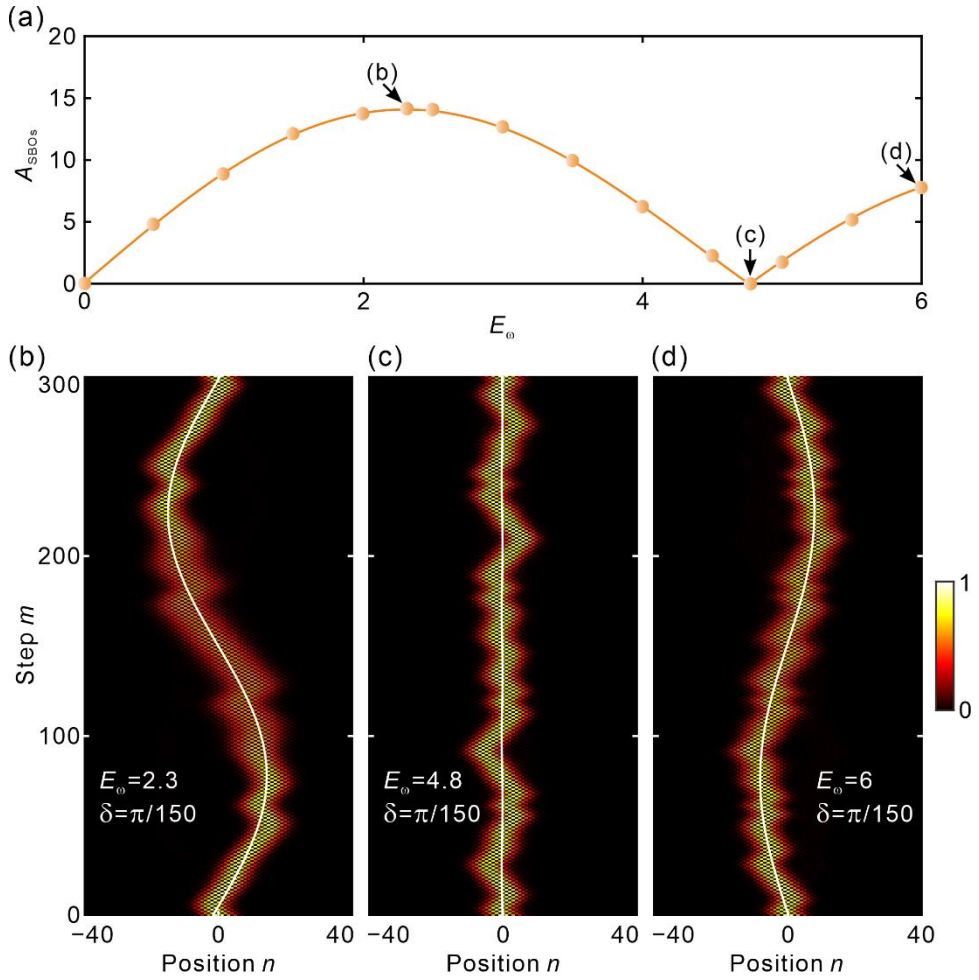

Fig. S3 Generalized SBOs under triangular-wave ac driving. (a) Oscillation amplitude A_{SBOs} varying with amplitude-to-frequency ratio E_ω. The solid curve and orange balls represent the theoretical and experimental results, respectively. (b)-(d) Simulated pulse intensity evolutions for $E_\omega = 2.3$, 4.8, and 6. The detuning is set as $\delta = \pi/150$.